PAPER • OPEN ACCESS

A novel index to evaluate CO2-induced wellbore cement degradation in CO2 rich environment

View the article online for updates and enhancements.

A novel index to evaluate CO₂-induced wellbore cement degradation in CO₂ rich environment

L W Zhang[1,2*], X X Miao[3], Y Wang[1], X W Cheng[4], K Ellett[5], M G Gan[1,2], X J Fu[1], S N Liu[1,2], X C Li[1,2]

[1]State Key Laboratory of Geomechanics and Geotechnical Engineering, Institute of Rock and Soil Mechanics, Chinese Academy of Sciences, Wuhan 430071, China
[2]University of Chinese Academy of Sciences, Beijing 100049, China
[3]State Key Laboratory for Geomechanics and Deep Underground Engineering, China University of Mining and Technology, Xuzhou 221116, China
[4]School of New Energy and Materials, Southwest Petroleum University, Chengdu 610500, China
[5]Indiana Geological and Water Survey, Indiana University, Bloomington 47405-2208, USA

*Corresponding author: lwzhang@whrsm.ac.cn

Abstract. A new index named CT-derived carbonation index is proposed to evaluate CO_2-induced cement degradation in CO_2-rich corrosive environment. This index is obtained by conducting CT scanning of cement samples before and after exposure to CO_2, calculating grayscale difference and applying an algorithm to correlate grayscale with $CaCO_3$ content. To demonstrate how to calculate the carbonation index, a CO_2–cement interaction experiment along with X-ray computed micro-tomography characterization of a cement sample before and after exposure to CO_2 was carried out to investigate the degree of cement carbonation. CO_2 was dissolved in 1 wt% NaCl solution under a CO_2 partial pressure of 17 MPa and a temperature of 63 °C. The carbonate shell in the cement sample was segmented from the grayscale difference images and the average penetration depth of the carbonate shell was obtained. The carbonation index was then calculated as the ratio of the average penetration depth of the carbonate shell to the radius of the sample, divided by the reaction time. In this study, the carbonation index of the cement sample exposed to CO_2 for 14 days was 0.01 day^{-1}. Based on the results in this study and other studies, a carbonation index of 0.05 day^{-1} or above corresponds to heavy degradation of cement by CO_2.

1. Introduction
From 1850 to nowadays, a substantial increase of global temperature has been recorded. The special IPCC report (2019) demonstrates that the mean land surface air temperature increased by about 1.5°C from 1850 to 2015 [1]. The rise of global temperature is directly related to anthropogenic CO_2 emissions, and carbon capture, utilization and storage (CCUS) is regarded as a viable technology to reduce CO_2 emissions. According to IEA Technology Roadmap, CCUS needs to account for 14% of CO_2 emission reduction to achieve the "2°C scenario" (i.e., the temperature rise is less than 2°C by 2050) [2].

Injection of CO_2 into deep subsurface lowers the pH of the CO_2 storage formation and introduces abundant dissolved inorganic carbon into the CO_2 storage formation, which may trigger wellbore cement degradation. A good approach to quantify wellbore cement degradation by CO_2 is to measure the penetration depth of the carbonate layer formed as a result of CO_2-cement reaction. Previous studies like [3-7] used SEM analysis to quantify carbonate layer thickness. However, SEM analysis is a 2D analysis technique and only one slice or several slices of a given sample can be analyzed, which limits the representativeness of the analysis results. Um et al. [8] used CT scanning to evaluate the level of carbonation for cement samples exposed to CO_2 and cement samples exposed to CO_2 + H_2S. However, their work only obtained raw CT images of cement samples after exposure to CO_2 and CO_2 + H_2S, and no post-processing of raw CT images was involved. Wan et al. used CT scanning to visualize and quantify carbonate layer thickness for cement samples exposed to CO_2 [9]. However, their study is in the field of concrete research and the reaction condition is low CO_2 concentration environment (i.e., the CO_2 partial pressure is 20% of the atmospheric pressure) [9]. In short, in the field of geologic CO_2 storage that involves very high CO_2 concentration (i.e., 10-30 MPa CO_2 partial pressure), no previous research has been done to post-process CT images of carbonated cement to reconstruct a 3D carbonate shell and use the penetration depth of the carbonate shell derived from CT imaging to determine the level of cement carbonation.

In this study, an experiment was carried out to immerse wellbore cement samples in an aqueous solution saturated with CO_2 (the solution was in equilibrium with supercritical CO_2 at a CO_2 partial pressure of 17 MPa and a temperature of 63ºC). X-ray CT imaging of the cement samples before and after the reaction was implemented to observe degradation and carbonation in cement samples. Through X-ray CT imaging, the penetration depth of the carbonate layer was obtained and an index named carbonation index derived from the penetration depth was proposed to evaluate the level of CO_2-induced carbonation in cement samples. The carbonation index proposed by this study is expected to have broad applications in the fields involving cementing under CO_2-rich environment, like CO_2-enhanced oil recovery, CO_2-rich natural gas production, geologic CO_2 storage, etc..

2. Methodology

A class G cement sample (10×30 mm cylinder with a 1mm diameter borehole at the center of the sample) was prepared and exposed to CO_2 saturated brine for 14 days under a CO_2 partial pressure of 17 MPa and a temperature of 63ºC, which mimicked typical geologic CO_2 storage conditions. An open borehole was made at the center of each sample to mimic a pre-existing CO_2 leakage pathway that is common in cement surrounding real wells. The sample before and after reaction with CO_2 was scanned by a Zeiss Xradia 410 Versa micro-CT scanner (Figure 1) and the raw CT images (Figure 2) went through a rigorous image registration, noise/artifact reduction and 3D reconstruction procedure. Details of this procedure can be found in [10]. After that, the carbonate content change at any location of the sample (locations are represented by voxels) after reaction with CO_2 was calculated by the following equation [10]:

$$\Delta f_{CC}^{t+1} = \frac{\lambda_{CC}\Delta\mu_E^{t+1}}{(-1-\lambda_{CC})\mu_{CH}+\mu_p+\lambda_{CC}\mu_{CC}} \tag{1}$$

where Δf_{CC}^{t+1} is the carbonate content change at a voxel from time t to time $t+1$; $\Delta\mu_E^{t+1}$ is the X-ray attenuation coefficient change at the voxel from time t to time $t+1$ (obtained from CT scanning data); λ_{CC} is the ratio of calcite volume increase to porosity reduction; μ_{CH}, μ_p and μ_{CC} represent the X-ray attenuation coefficients of pure $Ca(OH)_2$, pore (the same as the attenuation coefficient of air) and pure $CaCO_3$. The values of μ_{CH}, μ_p and μ_{CC} are available from literature search. The value of λ_{CC} depends on the dominant reaction occurring at the voxel. If the dominant reaction is $Ca(OH)_2$ dissolution by H^+, the value of λ_{CC} is 0. If the dominant reaction is $Ca(OH)_2$ displacement by $CaCO_3$, the value of λ_{CC} is

-369/38. If the dominant reaction is $CaCO_3$ precipitation (no $Ca(OH)_2$ displacement), the value of λ_{CC} is -1 [10].

The penetrating depth of the carbonate layer can then be derived from the carbonate content, and the penetrating depth is used to calculate the carbonation index, which is a cement carbonation level evaluation criterion proposed by this study:

$$I_c = \frac{1}{nt}\sum_{i=1}^{n}\frac{h_i}{r} \tag{2}$$

where I_c is carbonation index (day^{-1}); h_i is the CT image-derived penetration depth at location i (the locations are from bottom to top along the axis of the sample), note that the penetration depth at a given location is an averaged penetration depth that is derived from a 2D carbonate layer image from CT scanning; r is the radius of the sample, and h_i/r is called normalized penetration depth, which considers the influence of sample size; n is the number of locations considered along the axis of the sample; t is reaction time (day).

Figure 1. Zeiss Xradia 410 Versa micro-CT scanner used for sample analysis
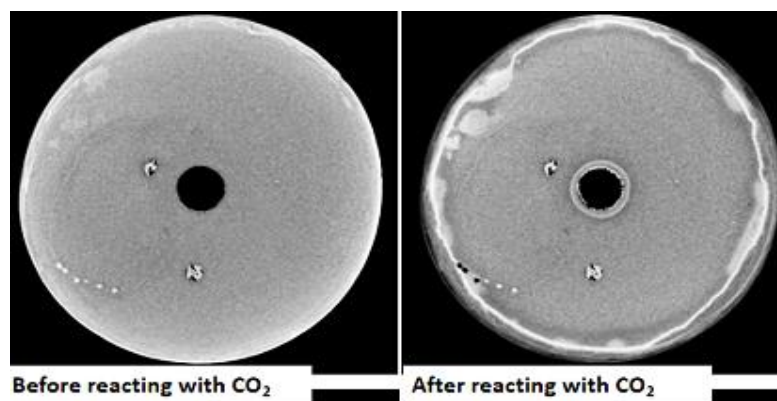

Figure 2. Raw CT images of the sample before and after reaction with CO_2 (cross-sectional slices)

3. Results and discussion

Figure 3 shows a 2D slice of grayscale intensity change of the cement sample after exposure to CO_2. The grayscale intensity change is normalized between -1 (maximum amount of dissolution) and 1 (maximum amount of precipitation). The blue ring in the image corresponded to the carbonate layer, which had low porosity. The ring outside the carbonate layer looked deep red (very porous) due to partial dissolution of $CaCO_3$. The ring inside the carbonate layer looked light red (slightly porous) due to dissolution of $Ca(OH)_2$ and amorphous calcium silicate hydrate (C-S-H) in cement. This "sandwich" pattern of layers is consistent with previous studies [4-5, 8]
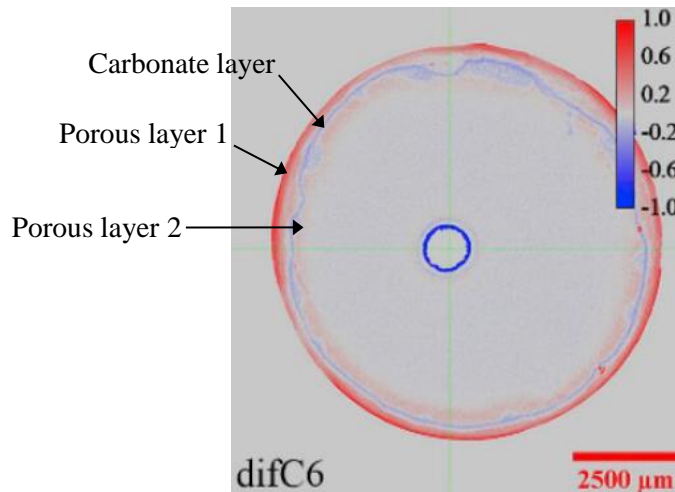

Figure 3. 2D grayscale intensity change of the sample after 14 days exposure to CO_2.

Figure 4a shows 3D $CaCO_3$ content distribution of the cement sample after exposure to CO_2. The mineral content change is normalized between -1 (maximum amount of dissolution) and 1 (maximum amount of precipitation). Most $CaCO_3$ was distributed within the inner borehole and close to the edge of the sample. More $CaCO_3$ precipitated within the inner borehole than near the edge of the sample, which was probably due to pH buffering of alkaline cement materials surrounding the inner borehole and the pH buffering favored $CaCO_3$ precipitation. Figure 4b shows the 3D skeleton of the $CaCO_3$ shell, which was derived from Figure 4a. The locations with brighter color represent higher $CaCO_3$ content. Because the cement sample was not homogeneous, the $CaCO_3$ shell formed was not homogeneous as well, with varying $CaCO_3$ contents at different locations. Figure 5 is a 2D slice of the $CaCO_3$ shell showing that the penetration depth of the $CaCO_3$ shell varied at different directions. For each 2D slice, an average $CaCO_3$ penetration depth was obtained by averaging 5-10 $CaCO_3$ penetration depths at different directions, and this average $CaCO_3$ penetration depth was the final penetration depth at the location where the slice was taken along Axis Z, as shown in Figure 5. For each location at Axis Z, there is an average $CaCO_3$ penetration depth, and the $CaCO_3$ penetration depths at 10 locations along Axis Z in the exterior and in the interior (at the borehole) are shown in Figure 6. Based on Equation (2), the carbonation index in the exterior of the sample is 0.01 day^{-1}, and the carbonate index in the interior of the sample is 5×10^{-4} day^{-1}. The carbonation index in the interior of the cement is much less than that in the exterior, because though there is heavy carbonation in the interior of the cement, $CaCO_3$ mainly accumulates within the borehole but does not penetrate much into the cement. As a result, the penetration depth in the interior of the cement is much less than that in the exterior.
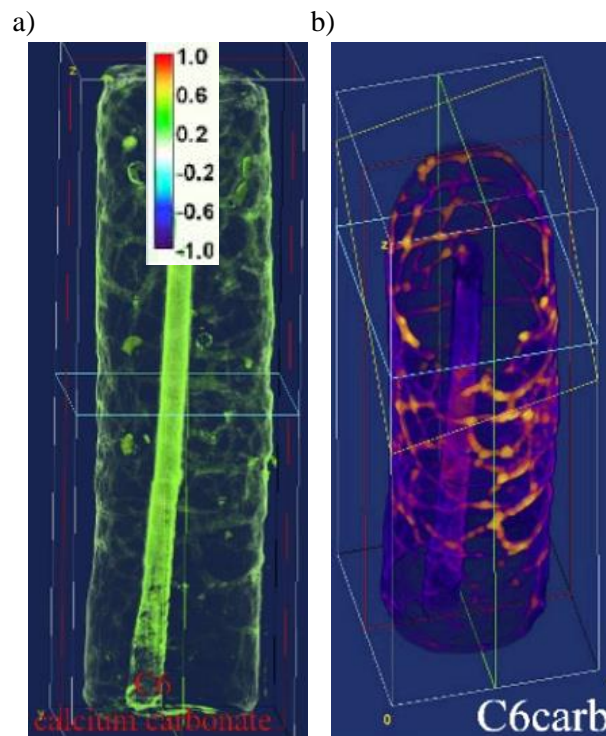
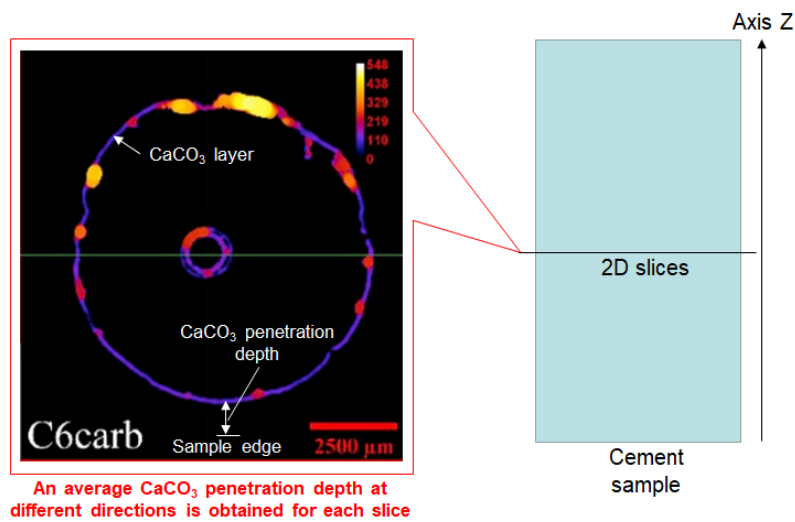**Figure 4.** $CaCO_3$ distribution of the cement sample after exposure to CO_2 (a) and the 3D skeleton of the $CaCO_3$ layer (b)

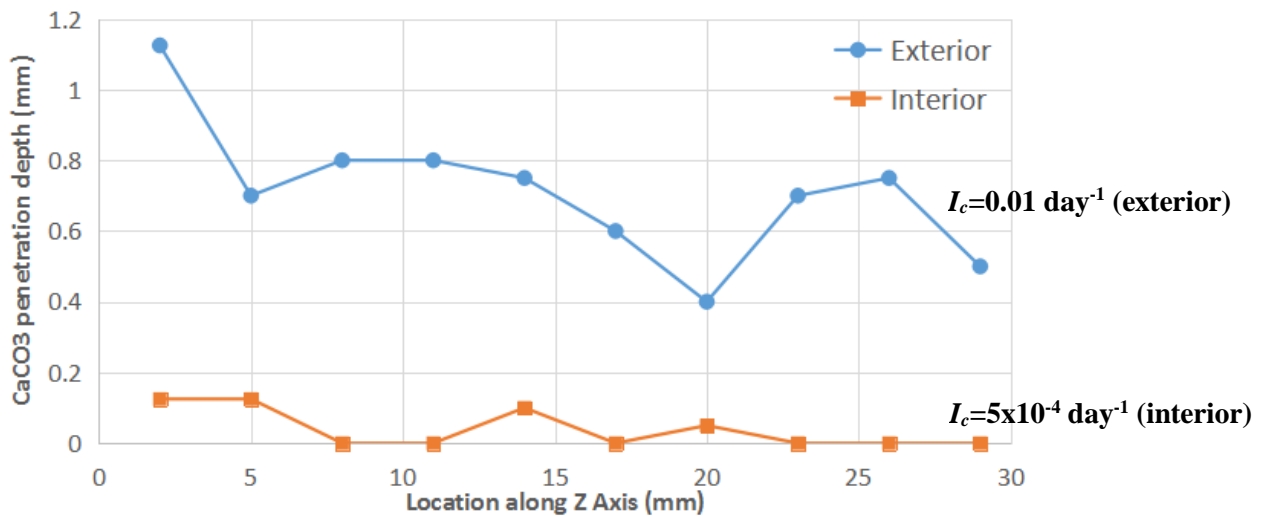**Figure 5.** A 2D slice of the $CaCO_3$ shell

Figure 6. Average $CaCO_3$ penetration depths at different locations along Z Axis of the sample

Based on the values of cement carbonation index in this and previous studies (Table 1), we propose the following criterion to determine the level of carbonation: negligible carbonation: < 0.001 day^{-1}; slight carbonation: 0.001-0.005 day^{-1}; moderate carbonation: 0.005-0.05 day^{-1}; heavy carbonation: > 0.05 day^{-1}.

Table 1. Values of cement carbonation index in this and previous studies

Literature	Carbonation index (day^{-1})	Level of carbonation
[3]	0.14 (Class G cement, 28 MPa CO_2 partial pressure)	Heavy
[3]	~0 (CO_2-resistent cement, 28 MPa CO_2 partial pressure)	Negligible
[4]	0.002 (Class H cement, 30.3 MPa CO_2 partial pressure)	Slight
[9]	~0 (Ordinary Portland cement, 0.02 MPa CO_2 partial pressure)	Negligible
[5]	0.003 (Class H cement + pozzolan additives, 12 MPa CO_2 partial pressure and 3.2 MPa H_2S partial pressure)	Slight
[6]	0.022 (Ordinary Portland cement, 10 MPa CO_2 partial pressure, without SO_4^{2-})	Moderate
[6]	0.015 (Ordinary Portland cement, 10 MPa CO_2 partial pressure, with SO_4^{2-})	Moderate
[8]	0.003 (Type I/II cement, 10 MPa CO_2 partial pressure)	Slight
This study	0.01 (Class G cement, 17 MPa CO_2 partial pressure)	Moderate

This index is applicable to cement or concrete samples exposed to very high CO_2 concentrations (i.e., CO_2 partial pressure higher than 1 MPa). For cement samples exposed to low CO_2 concentrations (i.e., CO_2 partial pressure lower than 1 MPa), this index always yields a result of negligible carbonation. Therefore, for low CO_2 concentration scenarios, the use of other indices to evaluate the level of carbonation is needed.

4. Conclusions

This study is the first to propose a carbonation index derived from CT scan images to evaluate CO_2-induced cement degradation in CO_2-rich corrosive environment. This index, based on CT scanning images, allows a comprehensive evaluation of cement carbonation and is more accurate than the penetration depth derived from SEM images in previous studies. A Class G cement sample was exposed to brine saturated with 17 MPa CO_2 under a temperature of 63ºC for 14 days in this study, yielding a carbonation index of 0.01 day^{-1}. Based on the values of cement carbonation index in this and previous studies, the following criterion to determine the level of cement carbonation is proposed: negligible carbonation: < 0.001 day^{-1}; slight carbonation: 0.001-0.005 day^{-1}; moderate carbonation: 0.005-0.05 day^{-1}; heavy carbonation: > 0.05 day^{-1}. The CT-derived carbonation index proposed by this study accurately evaluates the degree of cement carbonation under CO_2-rich environment.

5. References

[1] IPCC, Climate Change and Land: an IPCC special report on climate change, desertification, land degradation, sustainable land management, food security, and greenhouse gas fluxes in terrestrial ecosystems, 2019.
[2] IEA, IEA Technology Roadmap, 2019.
[3] Barlet-Gouedard V, Rimmelé G, Goffé B, Porcherie O 2007 *Oil Gas Sci. Technol.*, 62(3), 325-334.
[4] Kutchko B G, Strazisar B R, Lowry G V, Dzombak D A, Thaulow, N 2008 *Environ. Sci. Technol.*, 42(16), 6237-6242.
[5] Zhang L, Dzombak D A, Nakles D V, Hawthorne S B, Miller D J, Kutchko B G, Lopano C L, Strazisar B R 2014 *Int. J. Greenh. Gas Control*, 27, 299-308.
[6] Li Q, Lim Y M, Jun Y S 2015 *Environ. Sci. Technol.*, 49(11), 7032-7041.
[7] Nakano K, Mito S, Xue Z, Ohbuchi A J 2016 *Surf. Sci. Nanotechnol.*, 14, 198-203.
[8] Um W, Rod K A, Jung H B, Brown C F 2017 *Greenh. Gas Sci. Technol.*, 7(5), 852-865.
[9] Wan K, Xu Q, Wang Y, Pan, G 2014 *Cement Concrete Comp.*, 45, 255-263.
[10] Miao X, Zhang L, Wang Y, Wang L, Fu X, Gan M, Li, X 2020 *Cement Concrete Comp.*, 108, 103524.